

A Simple Explanation for the Observed Power Law Distribution of Line Intensity in Complex Many-Electron Atoms

Keisuke Fujii^{1, 2, *} and Julian C. Berengut^{3, 2}

¹*Department of Mechanical Engineering and Science,*

Graduate School of Engineering, Kyoto University, Kyoto 615-8540, Japan

²*Max-Planck-Institut für Kernphysik, Saupfercheckweg 1, 69117 Heidelberg, Germany*

³*School of Physics, University of New South Wales, New South Wales 2052, Australia*

(Dated: September 11, 2022)

It has long been observed that the number of weak lines from many-electron atoms follows a power law distribution of intensity. While computer simulations have reproduced this dependence, its origin has not yet been clarified. Here we report that the combination of two statistical models — an exponential increase in the level density of many-electron atoms and local thermal equilibrium of the excited state population — produces a surprisingly simple analytical explanation for this power law dependence. We find that the exponent of the power law is proportional to the electron temperature. This dependence may provide a useful diagnostic tool to extract the temperature of plasmas of complex atoms without the need to assign lines.

It has long been known that the the number of weak lines from many-electron atom in plasmas follows an intensity power law. In 1982 Learner pointed out this law for the first time when measuring emission lines from a hollow cathode lamp containing iron atoms [1]. He observed that the number density of lines with a given intensity I , $\rho_I(I)$, exhibits a power law dependence on I [2],

$$\rho_I(I) \propto I^{-1.50}. \quad (1)$$

He also reported that $\rho_I(I)$ in different wavelength regions all follow this power law with the same exponent, indicating an ergodic property of the emission line distribution [1].

This work has stimulated much discussion. A theoretical study by Scheeline showed that this power law does not hold for hydrogen atom spectra [3]. In contrast, the emission spectrum from arsenic, which has a much more complex electronic structure than hydrogen, shows closer distribution to the power law, but with a different value of the exponent [4]. Bauche-Arnoult and Bauche reported a simulation result with a collisional-radiative model for neutral iron atom and demonstrated that the power law dependence is again reproduced [5]. Their exponent was 17–25 % smaller than the Learner’s value but the reason was not clarified.

Pain recently reviewed this power law dependence problem and presented a discussion regarding fractal dimension and quantum chaos [6]. According to his discussion, the line strength distribution evaluated under the fully quantum-chaos assumption does not explain Learner’s law. As presented in his review, the origin of this power law has not been understood until now, though almost 40 years has been passed from the first report [6].

In this Letter, we present a surprisingly simple explanation of Learner’s law. We assume local thermal equilibrium of the excited state population, and an exponential

increase in the level density of complex atoms, which has been reported in several many-electron atoms and ions (e.g. [7, 8]). Combining these, we show below that the number of levels with a given population follows a power law distribution. An assumption of independently and identically distributed radiative transition rates then directly gives Learner’s law in the form

$$\rho_I(I) \propto I^{-2kT_e/\epsilon_0 - 1}, \quad (2)$$

where k is Boltzmann’s constant, T_e is electron temperature in the plasma, and ϵ_0 is the energy scale relating to the density of the excited states, which is ion-specific but does not depend on plasma parameters.

Plasma spectroscopy has been developed from simpler systems, e.g., hydrogen and rare gas atoms. It has been known that a comparison between intensity ratios of certain emission lines and collisional-radiative models provide us with information about plasma parameters, such as electron temperature and density [9–12]. This requires correct line identifications and accurate atomic data, e.g., energy levels and collision cross sections. However, accurate atomic data for open-shell atoms is difficult to obtain despite numerous demands for plasma diagnostics with complex atoms, ranging from laser produced plasmas for extreme-ultraviolet light sources [13–15], heavy metals contaminated fusion plasmas [16, 17], to the emissions found after the r -process supernova (kilonova) [18]. Our result Eq. (2) suggests an advantage of using intensity statistics for diagnosing plasmas with many-electron atoms, where accurate *ab initio* simulations of such complex spectra are still difficult with currently available theory and computers.

Next we derive Eq. (2), illustrating our assumptions using Learner’s example of neutral iron. Figure 1(a) shows the level density of neutral iron, $\rho_E(E)$, the number of levels with given excited energy E . This state density is evaluated from the experimentally measured energy levels taken from Atomic Spectral Database by National

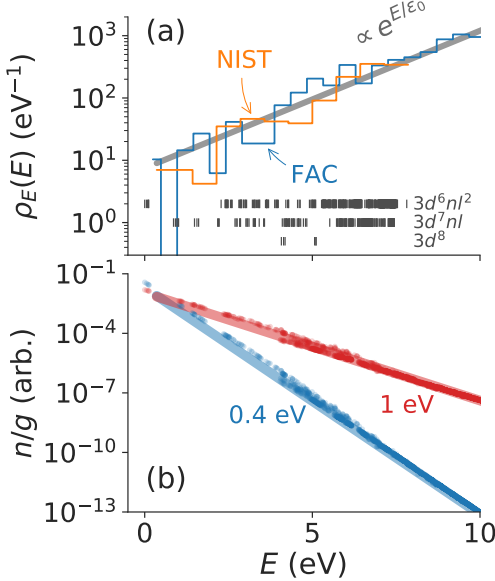


FIG. 1. (a) State density of neutral iron atom. The orange histogram is computed from the measurement data compiled in NIST ASD[19]. The measured energy levels (846 entries) are shown by the vertical bars in the figure. The blue histogram shows the state density computed from FAC [20]. The gray line is an exponential dependence Eq. (3) with $\epsilon_0 = 1.97$ eV, which fits both densities well. (b) Population distribution computed using collisional-radiative modelling with $T_e = 0.4$ eV (blue points) and 1 eV (red points) and electron density $n_e = 10^{20} \text{ m}^{-3}$. The blue and red bold lines present Boltzmann's distribution (Eq. (4)) with effective temperatures 0.38 and 0.8 eV, respectively.

Institute for Standard Technology [19]. The observed energy levels are shown by the vertical bars in the figure.

It is well known that the excited level density in the quantum many-body system increases nearly exponentially. One simple but common approximation is [8, 21, 22]

$$\rho_E(E) \propto \exp\left(\frac{E}{\epsilon_0}\right), \quad (3)$$

where ϵ_0 is an atom-specific energy scale. Dzuba *et al.* presented that for open-*d*- or *f*-shell atoms the state density follows Eq. (3) well enough at least below the ionization energy [8]. For the neutral iron, we find Eq. (3) well represents the level density with $\epsilon_0 \approx 1.97$ eV, as indicated by the solid line in Fig. 1(a).

Let us assume local thermal equilibrium for the excited state population. The population in state *i* with energy E_i is given as

$$n_i \propto g_i \exp\left(-\frac{E_i}{kT_e}\right), \quad (4)$$

where g_i is the statistical weight of the state *i* ($g_i =$

$2J_i + 1$, where J_i is the total angular momentum quantum number of state *i*). It has been known that this equilibrium is valid in high electron density and low electron temperature plasmas [10]. By substituting Eq. (3) into Eq. (4), the number of states having the population $n \sim n + dn$ can be written as,

$$\rho_n(n)dn = \rho_E(E)dn \propto \frac{1}{n} \rho_E(E)dn \quad (5)$$

$$\propto \frac{1}{n} \exp\left(-\frac{kT_e}{\epsilon_0} \log n\right) dn \quad (6)$$

$$\propto n^{-kT_e/\epsilon_0 - 1} dn, \quad (7)$$

where dE is the energy interval corresponding to dn , the relation of which can be obtained from Eq. (4). We assume in Eq. (6) that the statistical weight is distributed uniformly over the energy and therefore we omit it from the equation. This power law originates from the combination of the exponentially increasing one variable and exponentially decreasing another variable. This is a typical mathematical structure responsible to an emergence of power laws [23].

The emission intensity is proportional to the upper state population n_i , the cubic of transition energy $\omega_{ij}^3 = (E_i - E_j)^3$, and line strength S_{ij} , where *j* is the index of any lower states. In many-electron atoms with sufficient basis-state mixing, i.e., in quantum-chaotic systems, the probability distribution of S_{ij} can be well approximated as uniform and independent, and modeled using the Porter-Thomas distribution $p(S) \propto \frac{1}{\sqrt{2\pi S_0 S}} \exp(-\frac{S}{2S_0})$, with a constant S_0 [7, 24–26]. This approximation is obtained by modeling the Hamiltonian with a Gaussian orthogonal ensemble. As this distribution decays considerably faster than the power law, we can safely approximate that S_{ij} is a constant for all pairs of levels. Therefore, intensity I_{ij} is approximated as

$$I_{ij} \propto \omega_{ij}^3 S_0 n_i. \quad (8)$$

More detailed and precise discussion can be found in the Supplementary Material.

The number of emission lines from state *i* observed in photon energy range $\omega \sim \omega + \Delta\omega$ is proportional to the number of levels in this energy range, $\rho_E(E_i - \omega)d\omega$. By considering the number of emission lines with a given intensity range $I \sim I + dI$, we arrive at Eq. (2),

$$\rho_I(I)dI = \int_{\Omega} \rho_E(E - \omega) \rho_E(E) d\omega dE \propto I^{-2kT_e/\epsilon_0 - 1} dI \quad (9)$$

where the integration over ω is taken over the observed photon energy range, Ω . Here, the variable E is changed to I based on Eqs. Eq. (4) and Eq. (8). The factor 2 newly appears in the exponent of I compared with Eq. (7).

The exponent in Eq. (2) does not depend on Ω . This is consistent with Learner's observation that the emission

line density in different wavelength regions all show the power law dependence with the same exponent [1].

Learner suggested a relation between the exponent and a constant, $\log_{10} \sqrt{2}$ [1]. In contrast, our work clearly indicates a relation with T_e and an atom-specific constant ϵ_0 . By comparing the exponents in Eq. (1) and Eq. (2), the electron temperature in Learner's experiment is estimated as $(1.50 - 1)\epsilon_0/2 \approx 0.49$ eV, which is a reasonable electron temperature for a hollow cathode discharges with heavy atoms [5, 27, 28]. Bauche-Arnoult and Bauche have used $T_e = 0.4$ eV for their simulation [5], which is smaller than 0.49 eV. They obtained 1.392 ± 0.017 for the exponent [29], which is consistently smaller than Learner's value. Our above discussion further provides an explanation for one argument in their paper, i.e., higher the electron temperature, larger the exponent they obtained [5].

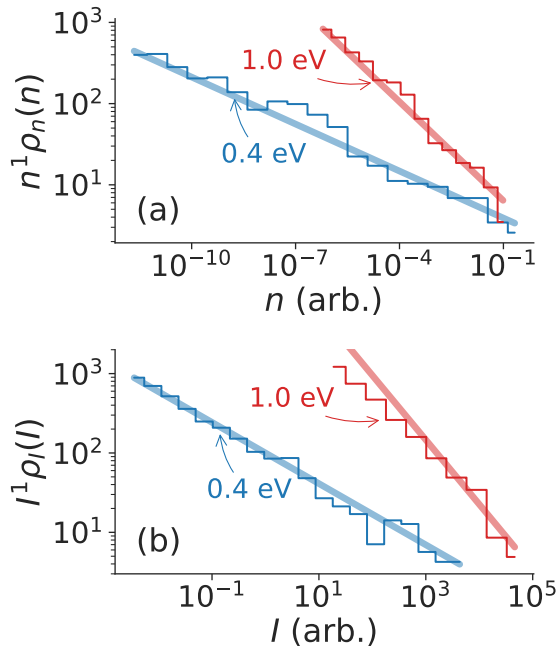


FIG. 2. (a) State density distribution $\rho_n(n)$, multiplied by n for visualization purpose. The blue histogram presents the computed result with $T_e = 0.4$ eV, while red presents the result with $T_e = 1$ eV. Both distributions follow the power law. (b) Density distribution of emission lines $\rho_I(I)$, computed by FAC. Again, the vertical values are multiplied by I to aid visualization. The bold lines in (a) and (b) are not fit results but theoretical models (Eqs. Eq. (7) and Eq. (2), respectively) with the same electron temperatures used in Fig. 1(b).

We carry out an *ab initio* simulation of the emission spectrum from neutral iron with the flexible atomic code (FAC) [20]. FAC uses the relativistic Hartree-Fock method to compute the electronic orbitals. Configuration interaction method is used to approximate the electron-electron interaction in the atoms. The popula-

tion and the emission line intensity are evaluated by the collisional-radiative model implemented in FAC, where the steady state of population in the plasma is assumed. For the collisional-radiative computation, we consider spontaneous emission, electron-impact excitation, deexcitation, and ionization, as well as the auto-ionization of the level above the ionization threshold, as elementary processes in plasmas. These rates are also calculated by FAC.

We assume $T_e = 0.4$ eV and the electron density $n_e = 10^{20} \text{ m}^{-3}$, as similar to Bauche-Arnoult and Bauche [5]. We also perform the simulation with $T_e = 1$ eV to observe the T_e dependence of the exponent. Note that in the FAC computations we do not explicitly assume either of the two assumptions, namely the exponential increase of the state density and the local thermal equilibrium of the population.

The state density of a neutral iron atom computed by FAC is shown in Fig. 1(a) by a blue step-line. It shows a similar exponential dependence to the measured data, NIST ASD. Figure 1(b) shows the excited state population computed by FAC. Although we do not assume local thermal equilibrium, the population follows the exponential function. The exponents for $T_e = 0.4$ and 1.0 eV cases are 0.38 eV and 0.8 eV, respectively, which are similar to the used temperature. Note that the slight difference between T_e and the exponent in the population is caused by a small violation of the local thermal equilibrium in plasma [10].

The histograms in Fig. 2(a) show the state density $\rho_n(n)$ with given population n (but scaled by n to aid visualization). The solid blue and red lines are computed according to Eq. (7) with $T_e = 0.38$ and 0.8 eV, respectively (the same temperatures used in Fig. 1(b)). Their agreement is clear.

Figure 2(b) shows the line intensity distribution $\rho_I(I)$, which appears in visible and infrared wavelength range (again scaled by I for visualization purpose). The solid lines show Eq. (2) with $T_e = 0.38$ and 0.8 eV for the two cases. This also agrees with the above discussion, particularly in the first three orders studied by Learner. In the low intensity region we see that $\rho_I(I)$ has systematically smaller values than the power law, particularly for the $T_e = 1.0$ eV case. Since only a limited number of excited states can be considered in the simulation, weaker emissions from the higher excited states that are far above the ionization energy are not included in the histogram. This is consistent with the fact that the deviation is larger in the higher T_e case, where more excited state population is generated.

In Eq. (2), we show that the exponent exclusively depends on T_e and ϵ_0 , but not on other atomic data, such as level energies, transition rates, and collision cross sections. The only value we require, ϵ_0 , is known to be accurately calculated with several atomic structure packages [8]. Therefore, Eq. (2) may be useful as a quick diagnostic

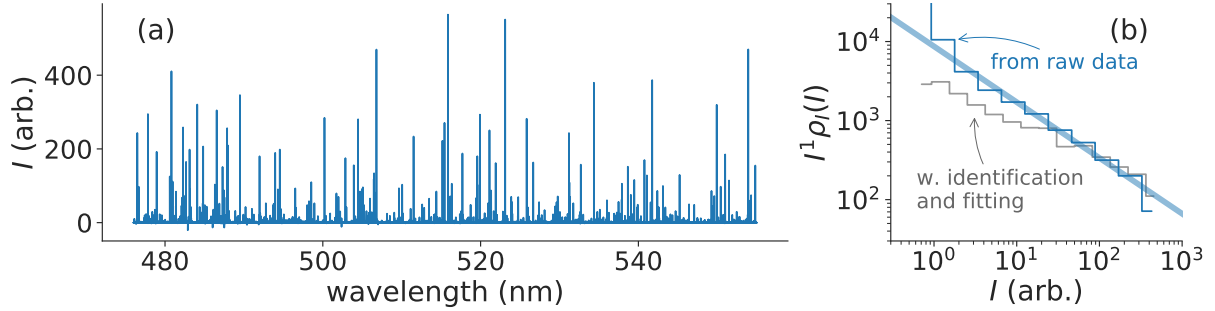


FIG. 3. (a) Emission spectrum observed from thorium-argon hollow cathode discharge [30, 31]. (b) Blue histogram: intensity directly computed from the spectrum in (a), without any calibration, line identification, and profile fitting. Gray histogram: intensity calculated after line identification and profile fitting. The solid line shows Eq. (2) with $T_e = 0.12$ eV.

method for many-electron atom plasmas.

As Eq. (2) is scale-free for I , the power law dependence is not affected by the system's sensitivity. Thus, any system calibration is not required for the T_e estimation. Furthermore, if the line width is considerably smaller than the instrumental function of the spectrometer and the instrumental function is well approximated by a Gaussian function, even the spectral fitting procedure to obtain the each line intensity is not necessary, because the wings of Gaussian decay faster than the power law and the contribution of the continuous line profile to the histogram is negligible. We only need to know the dominant (in terms of the number of emission lines) atom in the plasma.

Figure 3(a) shows a spectrum measured from a thorium-argon hollow cathode discharge by Palmer *et al.* [31, 32]. The dominant atom is neutral thorium, though there is finite contribution by singly and doubly charged thorium and argon atoms. We compute a histogram of this spectrum without any calibration, line identification and profile fitting. The result is shown by the blue histogram in Fig. 3(b). This histogram is in accordance with the power law. The gray histogram is derived from the emission line intensities of neutral thorium, which are identified based on the extensive line identification in the literature [30–32]. The intensity of each line is estimated by a standard procedure, i.e., by calibrating the wavelength, identifying lines, and fitting the line profiles by a Gaussian function. This histogram also shows a similar power law dependence, especially in the high intensity side. Note that its discrepancy in the lower intensity region is probably due to the contribution of yet unidentified lines.

The solid line in Fig. 3(b) shows Eq. (2) with $T_e = 0.12$ eV, where we use the value $\epsilon_0 \approx 0.68$ eV for neutral thorium by Dzuba *et al* [8]. This fits both the histogram computed directly from the raw spectrum and one from the line fitting (particularly in the high intensity side). Because there are no radiative rates reported for neutral thorium, it is difficult to estimate T_e for this plasma by

conventional methods. To our knowledge, the above procedure is the only one available to estimate T_e for thorium plasmas.

Although there are significant demands to diagnose plasmas with many-electron atoms, a quantitative comparison with an *ab initio* computer simulation model is not yet accurate enough, because of the unavailability of accurate atomic data. Our result suggests a possibility of plasma diagnostics that requires only the energy level statistics and the emission intensity statistics, though the validity condition of the local thermal equilibrium assumption should be investigated further. This may open the door to a statistical plasma spectroscopy.

In summary, we presented a simple explanation of Learner's law, where the histogram of the emission line intensities from many-electron atoms follows a power law. We observed that the exponent is analytically represented with T_e and ϵ_0 .

This work was partly supported by JSPS KAKENHI Grant Number 19K14680, and partly by the Max-Planck Society for the Advancement of Science. JCB is supported by the Alexander von Humboldt Foundation. We thank José Crespo Lopéz-Urrutia for useful discussions.

* fujii@me.kyoto-u.ac.jp

- [1] R. C. M. Learner, *Journal of Physics B: Atomic and Molecular Physics* **15**, L891 (1982).
- [2] Note that although he used a different base for the exponent, we present the converted value by $b \log 10 / \log 2 - 1$ for later convenience, where b is the original value, -0.15.
- [3] A. Scheeline, *Analytical Chemistry* **58**, 3103 (1986).
- [4] A. Scheeline, *Analytical Chemistry* **58**, 802 (1986).
- [5] C. Bauche-Arnoult and J. Bauche, *Journal of Quantitative Spectroscopy and Radiative Transfer* **58**, 441 (1997).
- [6] J.-C. Pain, *High Energy Density Physics* **9**, 392 (2013).
- [7] V. V. Flambaum, A. A. Gribakina, and G. F. Gribakin, *Physical Review A* **58**, 230 (1998).
- [8] V. A. Dzuba and V. V. Flambaum, *Physical Review Letters* **104**, 213002 (2010), arXiv:1003.4576.

[9] H. R. Griem, *Fast Electrical and Optical Measurements* (Springer Netherlands, Dordrecht, 1986) pp. 885–910.

[10] T. Fujimoto, *Plasma Polarization Spectroscopy* (Springer Berlin Heidelberg, Berlin, Heidelberg) pp. 29–49.

[11] K. Sawada, K. Eriguchi, and T. Fujimoto, *Journal of Applied Physics* **73**, 8122 (1993).

[12] M. Goto, *Journal of Quantitative Spectroscopy and Radiative Transfer* **76**, 331 (2003).

[13] N. Böwering, M. Martins, W. N. Partlo, and I. V. Fomenkov, *Journal of Applied Physics* **95**, 16 (2004).

[14] M. Masnavi, M. Nakajima, E. Hotta, K. Horioka, G. Niimi, and A. Sasaki, *Journal of Applied Physics* **101**, 033306 (2007).

[15] C. Suzuki, F. Koike, I. Murakami, N. Tamura, and S. Sudo, *Journal of Physics B: Atomic, Molecular and Optical Physics* **45**, 135002 (2012).

[16] T. Pütterich, R. Neu, R. Dux, A. D. Whiteford, and M. G. O'Mullane, *Plasma Physics and Controlled Fusion* **50**, 085016 (2008).

[17] I. Murakami, H. Sakaue, C. Suzuki, D. Kato, M. Goto, N. Tamura, S. Sudo, and S. Morita, *Nuclear Fusion* **55**, 093016 (2015).

[18] M. Tanaka, D. Kato, G. Gaigalas, P. Rynkun, L. Radžit, S. Wanajo, Y. Sekiguchi, N. Nakamura, H. Tanuma, I. Murakami, and H. A. Sakaue, *The Astrophysical Journal* **852**, 109 (2018), arXiv:1708.09101.

[19] A. Kramida, Y. Ralchenko, J. Reader, and N. A. T. (2018), “NIST Atomic Spectra Database (version 5.6.1),” (<https://physics.nist.gov/asd>), [Accessed: 8-Feb-2019].

[20] M. F. Gu, *Canadian Journal of Physics* **86**, 675 (2008).

[21] D. Ter Haar, *Physical Review* **76**, 1525 (1949).

[22] T. Von Egidy, A. N. Behkami, and H. H. Schmidt, *Nuclear Physics*, Tech. Rep. (1986).

[23] M. V. Simkin and V. P. Roychowdhury, *Physics Reports* **502**, 1 (2011).

[24] C. E. Porter and R. G. Thomas, *Physical Review* **104**, 483 (1956).

[25] S. M. Grimes, *Reexamination of she11 mode1 tests of the Porter-Thomas distribution*, Tech. Rep. 1 (1983).

[26] S. E. Bisson, E. F. Worden, J. G. Conway, B. Comaskey, J. A. D. Stockdale, and F. Nehring, *Journal of the Optical Society of America B* **8**, 1545 (1991).

[27] D. M. Mehs and T. M. Niemczyk, *Applied Spectroscopy* **35**, 66 (1981).

[28] L. Meng, R. Raju, R. Flauta, H. Shin, D. N. Ruzic, and D. B. Hayden, *Journal of Vacuum Science & Technology A: Vacuum, Surfaces, and Films* **28**, 112 (2010).

[29] This value is also converted from the original value $b = -0.118 \pm 0.005$.

[30] S. L. Redman, G. Nave, and C. J. Sansonetti, *The Astrophysical Journal Supplement Series* **211**, 4 (2014).

[31] “NIST Standard Reference Database 161,” <https://www.nist.gov/pml/spectrum-th-ar-hollow-cathode-lamps>, [Accessed: 27-Aug-2019].

[32] B. Palmer and R. J. Engleman, *Atlas of the thorium spectrum*, Tech. Rep. (Los Alamos National Laboratory (LANL), Los Alamos, NM, 1980).

A Simple Explanation for the Observed Power Law Distribution of Line Intensity in Complex Many-Electron Atoms

In the main text, we used “ \propto ” in most of the equations and ignored constant factors (e.g., Eqs. 2, 3, and 6) to simplify the discussion. Furthermore, we made a rather drastic approximation in Eq. (8): the constant radiative transition rate. In this Supplemental Material, we present explicit formulae and explain the approximation in more detail. As we will see later, even if we consider the probability distribution of the transition rate, we arrive at the same result.

Let us redefine explicitly the level density $\rho_E(E)$ and the population n_i at state i having the excited energy E_i as follows,

$$\rho_E(E) = \rho_0 \exp\left(\frac{E}{\epsilon_0}\right), \quad (S1)$$

and

$$n_i = n_0 \bar{g} \exp\left(-\frac{E_i}{kT_e}\right), \quad (S2)$$

where ρ_0 and n_0 are constants. \bar{g} is the averaged statistical weight for all the state, which we assumed constant over all the levels in the main text. The distribution of g_i does not affect the result as long as the distribution is uniform and independent of energy.

The number of states having the population $n \sim n + dn$ can be written as

$$\rho_n(n)dn = \rho_E(E)dE = \frac{kT_e}{n} \rho_E(E)dn \quad (S3)$$

$$= \frac{kT_e}{n} \rho_0 \exp\left(-\frac{kT_e}{\epsilon_0} (\log n - \log n_0 - \log \bar{g})\right) dn \quad (S4)$$

$$= \rho_0 kT_e (n_0 \bar{g})^{kT_e/\epsilon_0} n^{(-kT_e/\epsilon_0 - 1)} dn \quad (S5)$$

Let us consider the number of emission lines found in the photon energy range of $\omega \sim \omega + d\omega$ from level i with $0 \leq \omega \leq E_i$. Because of the finite wavefunction mixing, the number of emission lines equals to the number of levels within $E_i - (\omega + d\omega) \sim E_i - \omega$, which is $\rho_E(E - \omega)d\omega$. The number of emission lines from the excited states existing within the excited energy $E \sim E + dE$ is

$$L(E, \omega)d\omega dE = \rho_E(E - \omega)d\omega \rho_E(E)dE \quad (\text{S6})$$

$$= \rho_0^2 \exp\left(\frac{2E - \omega}{\epsilon_0}\right) d\omega dE \quad (\text{S7})$$

The intensity of the emission line corresponding to the transition from the state i to state j , I_{ij} , is written as $I_{ij} = A_{ij}n_i$, where A_{ij} is the radiative transition rate from state i to state j . A_{ij} relates to the line strength S_{ij} , $A_{ij} = \gamma\omega_{ij}^3 S_{ij}$, with $\omega_{ij} = E_i - E_j$ and $\gamma = \frac{16\pi^3 e^2}{3\nu_0 h^4 c^3}$, with e the elementary charge, ν_0 vacuum permittivity, h Planck's constant, and c light speed.

In order to simplify the discussion, at this moment, let us assume A_{ij} has a solid relation $A_{ij} = \gamma\omega_{ij}^3 S_0$ for all i and j pairs with a constant S_0 , and relax this assumption later. Then, the intensity only depends on the population of state i . The number of lines with given intensity I_c , with this constant assumption is

$$\rho_{I_c}(I_c, \omega)dI_c d\omega = L(E, \omega)dEd\omega \quad (\text{S8})$$

$$= \rho_0^2 \exp\left(-\frac{\omega}{\epsilon_0}\right) \exp\left(-2\frac{kT_e}{\epsilon_0} \log\left(\frac{I_c}{\omega^3 \gamma S_0 n_0 \bar{g}}\right)\right) \frac{kT_e}{I_c} dI_c d\omega \quad (\text{S9})$$

$$= \rho_0^2 \exp\left(-\frac{\omega}{\epsilon_0}\right) (\omega^3 \gamma S_0 n_0 \bar{g})^{(2kT_e/\epsilon_0)} kT_e I_c^{(-2kT_e/\epsilon_0 - 1)} dI_c d\omega, \quad (\text{S10})$$

where dI_c is the intensity range that corresponds to the energy range dE , which can be found from Eq. S2 and $I_c = \omega^3 \gamma S_0 n$. Note here already that the dependence of I_c in the distribution follows the final distribution (Eq. 2).

Now we relax the constant line strength assumption and consider the stochastic nature of S_{ij} . Let \tilde{s} be the fluctuation in S , $S = \tilde{s}S_0$. The probability distribution of \tilde{s} may be written as $p_{\tilde{s}} = \frac{1}{\sqrt{2\pi\tilde{s}}} \exp(-\tilde{s}/2)$, which is a Poer-Thomas distribution with mean 1 [7, 24–26]. As we will see later, the actual shape of $p_{\tilde{s}}$ is not important as long as it decays exponentially in large \tilde{s} limit. More importantly, we here assume that $p_{\tilde{s}}$ is independent and identical for all the transitions. With this assumption, the intensity I becomes a product of two independent random variables, $I = \tilde{s}I_c$.

Let us consider only the probability distribution of I_c , rather than the number of lines. Since the distribution of I_c follows the power law, the probability distribution of I_c is written as a Pareto distribution,

$$p_{I_c}(I_c) = \alpha I_{\min}^\alpha I_c^{-\alpha-1} \quad (\text{s.t. } I_c \geq I_{\min}) \quad (\text{S11})$$

where $\alpha = 2kT_e/\epsilon_0$ and I_{\min} is the minimum value of the intensity. We will take a limit of $I_{\min} \rightarrow 0$ later but in order to make the distribution integrable, we now assume this value is sufficiently small. The probability distribution of the intensity is written as

$$p(I|\omega) = \int_0^\infty p_{\tilde{s}}(\tilde{s}) p_{I_c}(I/\tilde{s}) \frac{1}{\tilde{s}} d\tilde{s} \quad (\text{S12})$$

$$= \alpha I_{\min}^\alpha I^{(-\alpha-1)} \int_0^{I/I_{\min}} \tilde{s}^\alpha p_{\tilde{s}}(\tilde{s}) d\tilde{s}. \quad (\text{S13})$$

If $p_{\tilde{s}}(\tilde{s})$ decays faster than $\tilde{s}^{-\alpha-1}$ (such as the exponential decay) and $I \gg I_{\min}$, the integral in the right hand side converges and does not depend on I . With sufficiently small I_{\min} (which corresponds to sufficiently large E for the upper state), $p(I|\omega)$ becomes the power law distribution except for the very small I region. This distribution actually has the same shape as Eq. (S8) where we assume that S is constant.

Let us consider the sensitivity of the observation system, $\xi(\omega)$. The density distribution of the observed intensity $I' = \xi(\omega)I$ is

$$\rho_{I'}(I')dI' = \rho_0^2 \exp\left(-\frac{\omega}{\epsilon_0}\right) (\omega^3 \gamma S_0 n_0 \bar{g} \xi(\omega)^{-1})^{(2kT_e/\epsilon_0)} kT_e I'^{(-2kT_e/\epsilon_0 - 1)} dI'. \quad (\text{S14})$$

The system's sensitivity only affects the scale of the distribution, but not the exponent of the power law.

A histogram may be computed from an emission spectrum observed in finite wavelength range, Ω . It corresponds to the integration of Eq. (S14) over the observation wavelength range,

$$\int_{\Omega} d\omega \rho_{I'}(I') d\omega dI' \propto I'^{-2kT_e/\epsilon_0 - 1} dI' \quad (\text{S15})$$

which results in the same power law. Therefore, no system calibration is necessary to compute the intensity histogram. This ergodic property essentially comes from the fact that the power law is scale invariant.